

A time dependent thermal and solutal convection problem in physical vapor transport of $\text{Hg}_2\text{Cl}_2\text{-I}_2$ system

Geug Tae Kim[†]

Department of Advanced Materials and Chemical Engineering, Hannam University, Daejeon 34054, Korea

(Received February 23, 2017)

(Revised March 17, 2017)

(Accepted March 24, 2017)

Abstract In this research a time dependent thermal and solutal convection was computationally investigated for the physical vapor transport of the mixture of $\text{Hg}_2\text{Cl}_2\text{-I}_2$ system with for the convective regime from thermal Rayleigh number of 2.16×10^6 up to 1.7×10^7 with marching time to a steady state problem. With time marching, the convective cells are decreased for the thermal Rayleigh number of 2.16×10^6 , and increased for the thermal Rayleigh number of 1.7×10^7 . The convective flow structures are found to be essentially time independent on the horizontal orientation of the enclosure with respect to the gravity vector, and on the other hand, time dependent on the vertical orientation of the enclosure with respect to the gravity vector.

Key words Time dependent, Convection

1. Introduction

This paper concerns the time dependent thermal and solutal convection problems, which arise from the physical vapor transport processes of the mixture of $\text{Hg}_2\text{Cl}_2\text{-I}_2$ system to predict the transition from unsteady to steady state flows. These problems are primarily of two configurations of enclosures. Firstly, there is the configuration of the horizontal position, i.e., horizontal temperature and solutal gradients present in the system of horizontal rectangular geometry with differentially heated end walls. Secondly, with respect to a vertical position, when the source material of mercurous chloride (Hg_2Cl_2) is placed with a furnace imposed with a linear temperature profile, the source of mercurous chloride sublimates and is transported as a mixture of Hg_2Cl_2 vapor and impurity of I_2 and is recrystallized into the crystal region. In this study, the latter problem is focused because it has essentially the time dependent thermal and solutal problem under convective parameter ranges. In a view of point of stabilizing temperature profiles, the former problem is also covered in a case chosen for the study of the convective flow structure.

Duval investigated systematically for a wide range of convective parameters of thermal Rayleigh number from 1.80×10^1 to 5.03×10^7 [1-4]. In particular,

Duval investigate computationally the time dependent problems in refs [1-4]. Until now, much research are focused into the problems at the steady state during the physical vapor transport (PVT) processes [5-10]. With regard to studies on the PVT in the vapor phase, in a more recent year Tebbe et al. [12] extended for transition to chaos flow fields in specialty materials of mercurous chloride in applications of microgravity experiments. In this study, one uses a material of Hg_2Cl_2 as a model sample and investigate numerically the influence of gravitational accelerations on diffusive convection during the PVT of a mixture of Hg_2Cl_2 vapor and impurity of I_2 . The distinction of this study in a comparison with our previous study [13] is centered into the unsteady state problem with thermal and solutal convection problems in both a vertical and a horizontal position with respect to the gravity. Therefore, in this study, the detailed convective flow structures are discussed in the transition from unsteady state to steady state.

2. Numerical Analysis

A detailed understanding of the convective structures as well as the transition from the time dependent state to steady state is required since crystal quality is significantly affected by convection, and particularly for the growth of high quality crystals, the flow oscillations due to the time dependent convective flow should

[†]Corresponding author
E-mail: geugtaekim@gmail.com

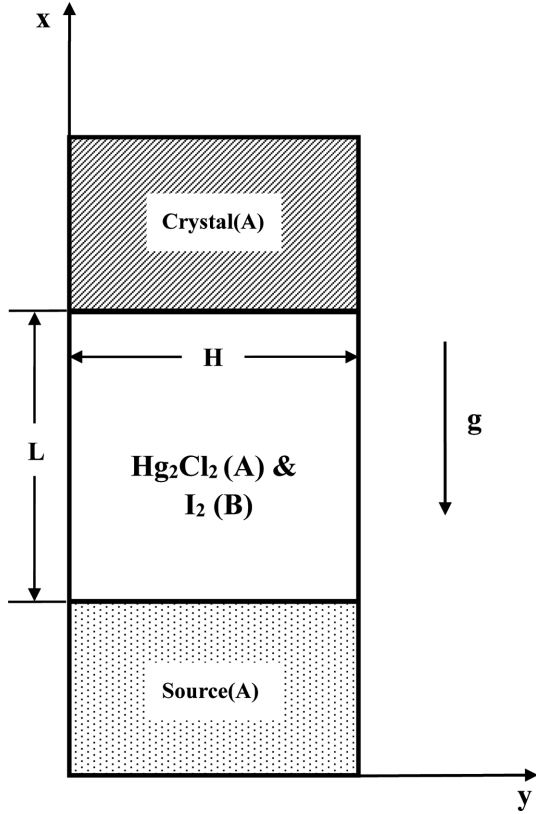


Fig. 1. Schematic description of a two-dimensional PVT model for a $\text{Hg}_2\text{Cl}_2\text{-I}_2$ system in a vertical position.

be avoided. Therefore, one restricts one's model to examine how a typical thermal and solutal convective flow fields advance with marching time. For this study, a time dependent model will be sufficient. As shown in Fig. 1, one has used to a rectangle to represent the ampoule with a source of and a crystal of material Hg_2Cl_2 on the two differentially heated ends. An aspect ratio (transport length L to height H) of 1 is considered with the source temperature T_s and the crystal temperature T_c , with $T_s > T_c$.

One assumes thermodynamic equilibrium at the interfaces, the mass fraction are fixed. For an incompressible fluid, the governing equations of mass (continuity), momentum, energy and species (diffusion) may be expressed as follow [4]:

$$\nabla \cdot \vec{V} = 0, \quad (1)$$

$$\rho \frac{D\vec{V}}{Dt} = -\nabla p + \mu \nabla^2 \vec{V} + \rho \vec{g}, \quad (2)$$

$$\frac{DT}{Dt} = \alpha \nabla^2 T, \quad (3)$$

$$\frac{D\omega_A}{Dt} = D_{AB} \nabla^2 \omega_A. \quad (4)$$

With the following initial and boundary conditions [4]:

Initial conditions:

$$\text{time } t = 0; 0 < x < L, 0 < y < H.$$

Boundary conditions:

On the walls ($0 < x < L, y = 0$ and H):

$$u(x, 0) = u(x, H) = v(x, 0) = v(x, H) = 0,$$

$$\frac{\partial \omega_A(x, 0)}{\partial y} = \frac{\partial \omega_A(x, H)}{\partial y} = 0,$$

$$T(x, 0) = T(x, H) = \frac{T - T_c}{T_s - T_c}.$$

On the source ($x = 0, 0 < y < H$):

$$u(0, y) = -\frac{D_{AB}}{(1 - \omega_{A,c})} \frac{\partial \omega_A(0, y)}{\partial x},$$

$$v(0, y) = 0,$$

$$T(0, y) = T_s,$$

$$\omega_A(0, y) = \omega_{As}.$$

On the crystal ($x = L, 0 < y < H$):

$$u(L, y) = -\frac{D_{AB}}{(1 - \omega_{A,s})} \frac{\partial \omega_A(L, y)}{\partial x},$$

$$v(L, y) = 0,$$

$$T(L, y) = T_c,$$

$$\omega_A(L, y) = \omega_{Ac}.$$

These equations are solved using a SIMPLER (Semi-Implicit Method for Pressure-Linked Equation Revised) algorithm with a one-time per time step method, which is sometimes used to obtain the steady state solution at the end of many time steps [14, 15]. One uses a 52×52 grid size system for all the cases.

3. Results and Discussion

Both thermal and solutal convection become important because the molecular weights of the mercurous chloride vapor (A) and iodine vapor (B) are unequal. For the binary system under consideration in this study, mercurous chloride ($M_A = 472.8$) and iodine ($M_B = 253.8$), the solutal Rayleigh number dominates over the thermal Rayleigh number. For the case when the ampoule is placed in the vertical position with a vertical temperature differences of 50 K and 70 K between the source and the crystal ends, i.e., the hot temperature at the bottom and the cold temperature at the top, which indicates the destabilizing temperature field, the

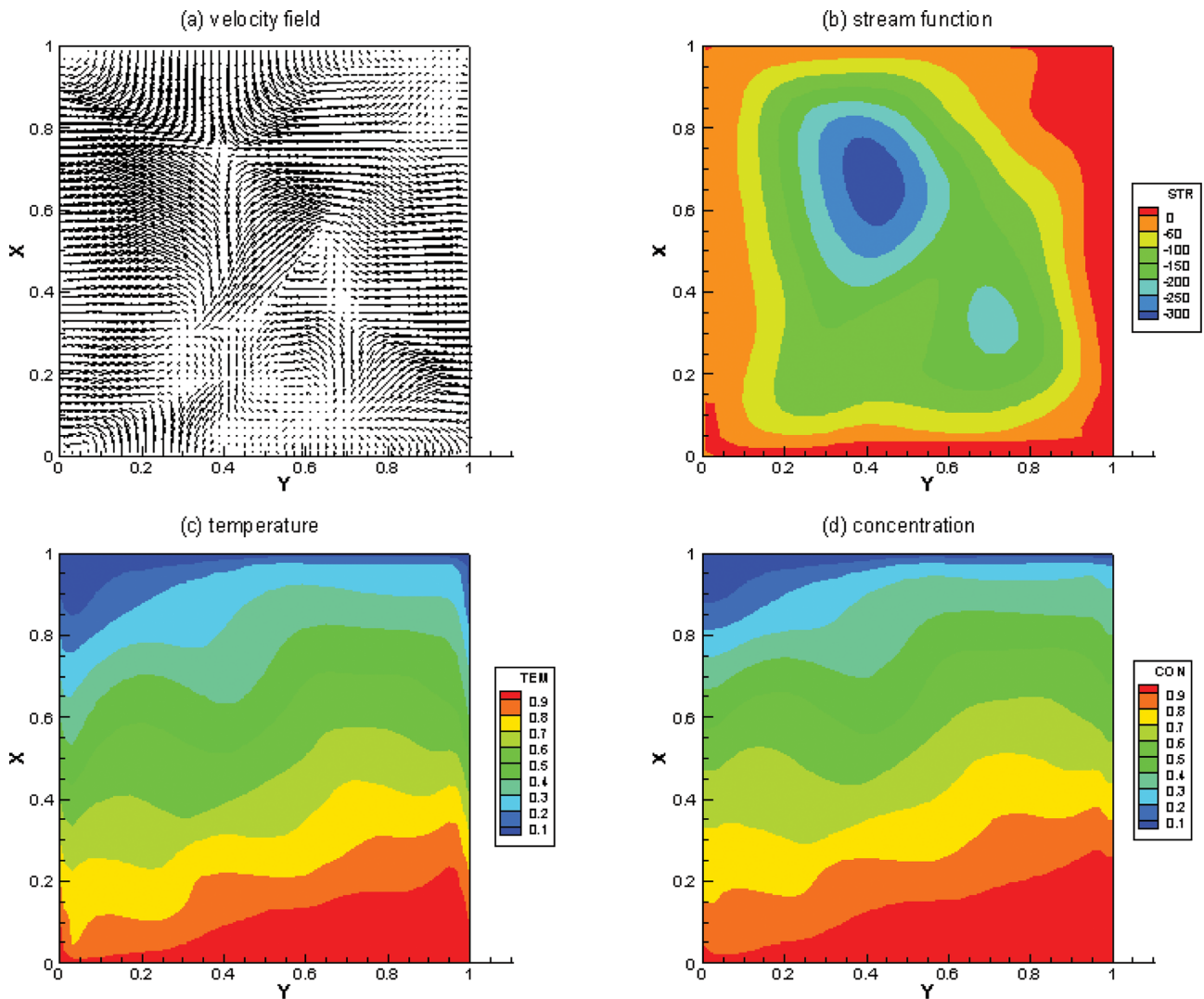


Fig. 2. Convective structures of velocity field, stream function, temperature and concentration at time (t) = 10,000 seconds. Based on aspect ratio (Ar) = 1, transport length $L = 10$ cm, a linear wall temperature profile between $T_s = 623$ K and $T_c = 573$ K, thermal Rayleigh number (Ra_t) = 1.34×10^7 , solutal Rayleigh number (Ra_s) = 6.6×10^7 , Prandtl number (Pr) = 1.16, Lewis number (Le) = 0.7, Peclet number (Pe) = 1.82, concentration parameter = 1.19, partial pressure of impurity (I_2) = 100 Torr. (a) velocity field, (b) stream function ($\Delta\psi = 50$, $\psi_{max} = 30.6$, $\psi_{min} = -331$), (c) temperature ($\Delta T = 0.1$, $T_{max} = 1.0$, $T_{min} = 0$), (d) concentration ($\Delta C = 0.1$, $C_{max} = 1.0$, $C_{min} = 0$). A relative velocity vector with a magnitude of 1,000 has 0.5 cm. The maximum velocity vector is 6.99 cm s^{-1} .

concentration field becomes stabilizing due to the thermodynamic constraints. As shown in Figs. 2 and 3, even if the temperature field is destabilizing, since the solutal Rayleigh number is greater than the thermal Rayleigh number by one order of magnitude, the system of interest is reduced to be stable. As the time advances from 10,000 seconds to 30,000 seconds, the convective structure is transited to two convective cells into one single convective cell, which the flow field is stabilized with marching time, and results in one single cell at the steady state. Fig. 2 shows the convective structures of velocity field, stream function, temperature and concentration at $t = 10,000$ seconds, based on aspect ratio (Ar) = 1, transport length

$L = 10$ cm, a linear wall temperature profile between $T_s = 623$ K and $T_c = 573$ K, thermal Rayleigh number (Ra_t) = 1.34×10^7 , solutal Rayleigh number (Ra_s) = 6.6×10^7 , Prandtl number (Pr) = 1.16, Lewis number (Le) = 0.7, Peclet number (Pe) = 1.82, concentration parameter = 1.19, partial pressure of impurity (I_2) = 100 Torr. The (a) velocity field, (b) stream function ($\Delta\psi = 50$, $\psi_{max} = 30.6$, $\psi_{min} = -331$), (c) temperature ($\Delta T = 0.1$, $T_{max} = 1.0$, $T_{min} = 0$), (d) concentration ($\Delta C = 0.1$, $C_{max} = 1.0$, $C_{min} = 0$) are given. In addition, a relative velocity vector with a magnitude of 1,000 has 0.5, with the maximum velocity vector of 6.99 cm s^{-1} . Fig. 3 shows the convective structures of velocity field, stream function, temperature and concentration at $t = 30,000$

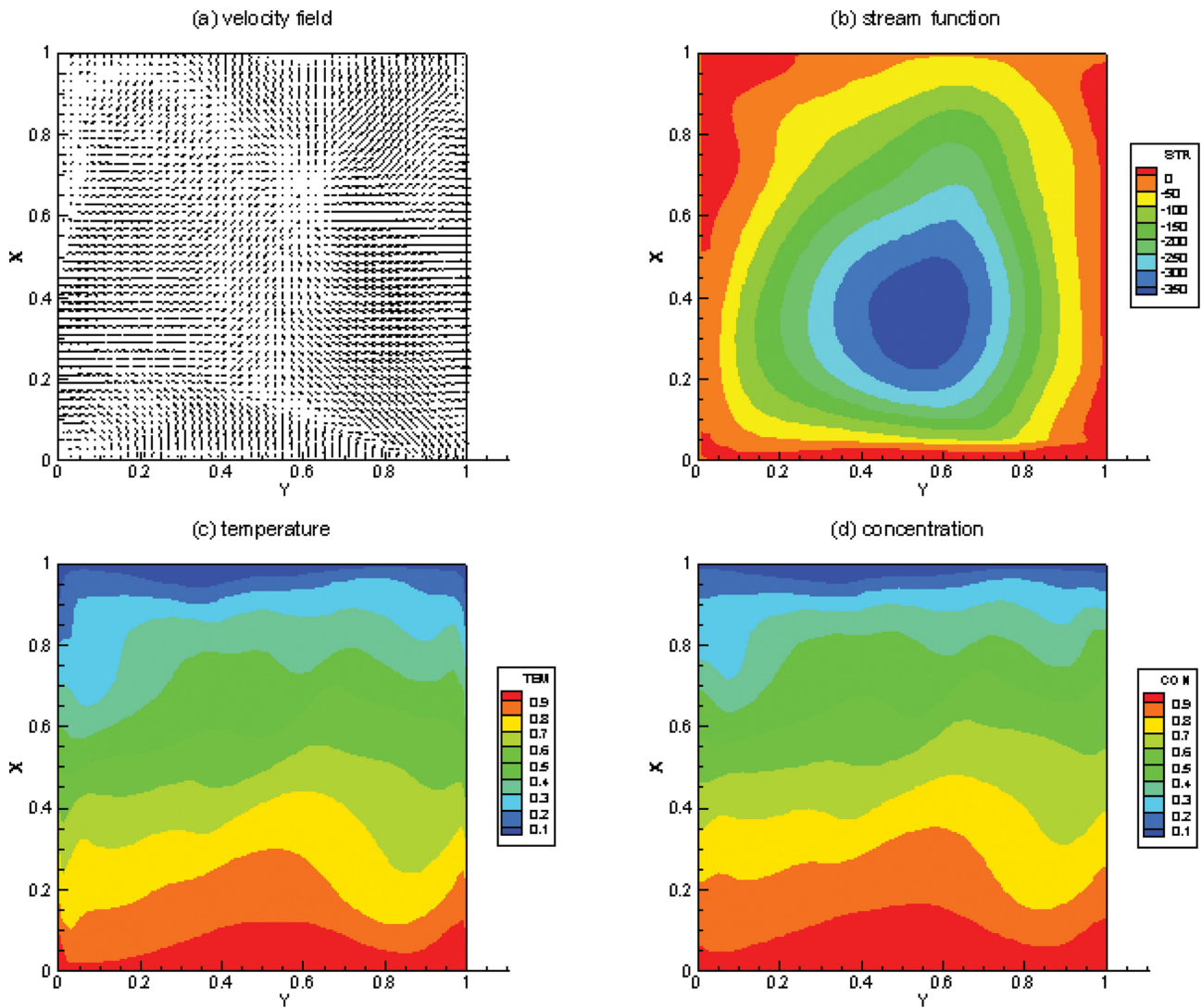


Fig. 3. Convective structures of velocity field, stream function, temperature and concentration at time $(t) = 30,000$ seconds. (a) velocity field, (b) stream function ($\Delta\psi = 50$, $\psi_{\max} = 39.8$, $\psi_{\min} = -391$), (c) temperature ($\Delta T = 0.1$, $T_{\max} = 1.0$, $T_{\min} = 0$), (d) concentration ($\Delta C = 0.1$, $C_{\max} = 1.0$, $C_{\min} = 0$). A relative velocity vector with a magnitude of 1,000 has 0.2 cm. The maximum velocity vector is 7.01 cm s^{-1} .

seconds: (a) velocity field, (b) stream function ($\Delta\psi = 50$, $\psi_{\max} = 39.8$, $\psi_{\min} = -391$), (c) temperature ($\Delta T = 0.1$, $T_{\max} = 1.0$, $T_{\min} = 0$), (d) concentration ($\Delta C = 0.1$, $C_{\max} = 1.0$, $C_{\min} = 0$). A relative velocity vector with a magnitude of 1,000 has 0.2 cm, with the maximum velocity vector of 7.01 cm s^{-1} . For the two cases of times of 10,000 and 30,000 seconds, the magnitude of the maximum velocities are nearly invariant and of same order of magnitude. As shown in Fig. 3(a) velocity field, (b) stream function, (c) temperature, (d) concentration, the convective flow fields are symmetrical; on the other hand, as shown in Fig. 2(a) velocity field, (b) stream function, (c) temperature, (d) concentration, the convective flow fields are asymmetrical.

Figs. 4 and 5 concern the convective flow struc-

tures when the thermal Rayleigh number is further increased from 1.34×10^7 to 1.7×10^7 , i.e. the temperature difference between the source and the crystal, $\Delta T = 50 \text{ K} \rightarrow 70 \text{ K}$. The convective structures are switched from one single cell over three convective cells when the thermal Rayleigh number is increased under the thermal Rayleigh number ranges ($1.34 \times 10^7 \sim 1.7 \times 10^7$) under consideration. As shown in Figs. 4 and 5, for the both cases, the convective structures are asymmetrical. Fig. 4 shows the convective structures of velocity field, stream function, temperature and concentration at $t = 10,000$ seconds, based on aspect ratio = 1, transport length $L = 10 \text{ cm}$, a linear wall temperature profile between $T_s = 623 \text{ K}$ and $T_c = 553 \text{ K}$, thermal Rayleigh number $(Ra_t) = 1.7 \times 10^7$, solu-

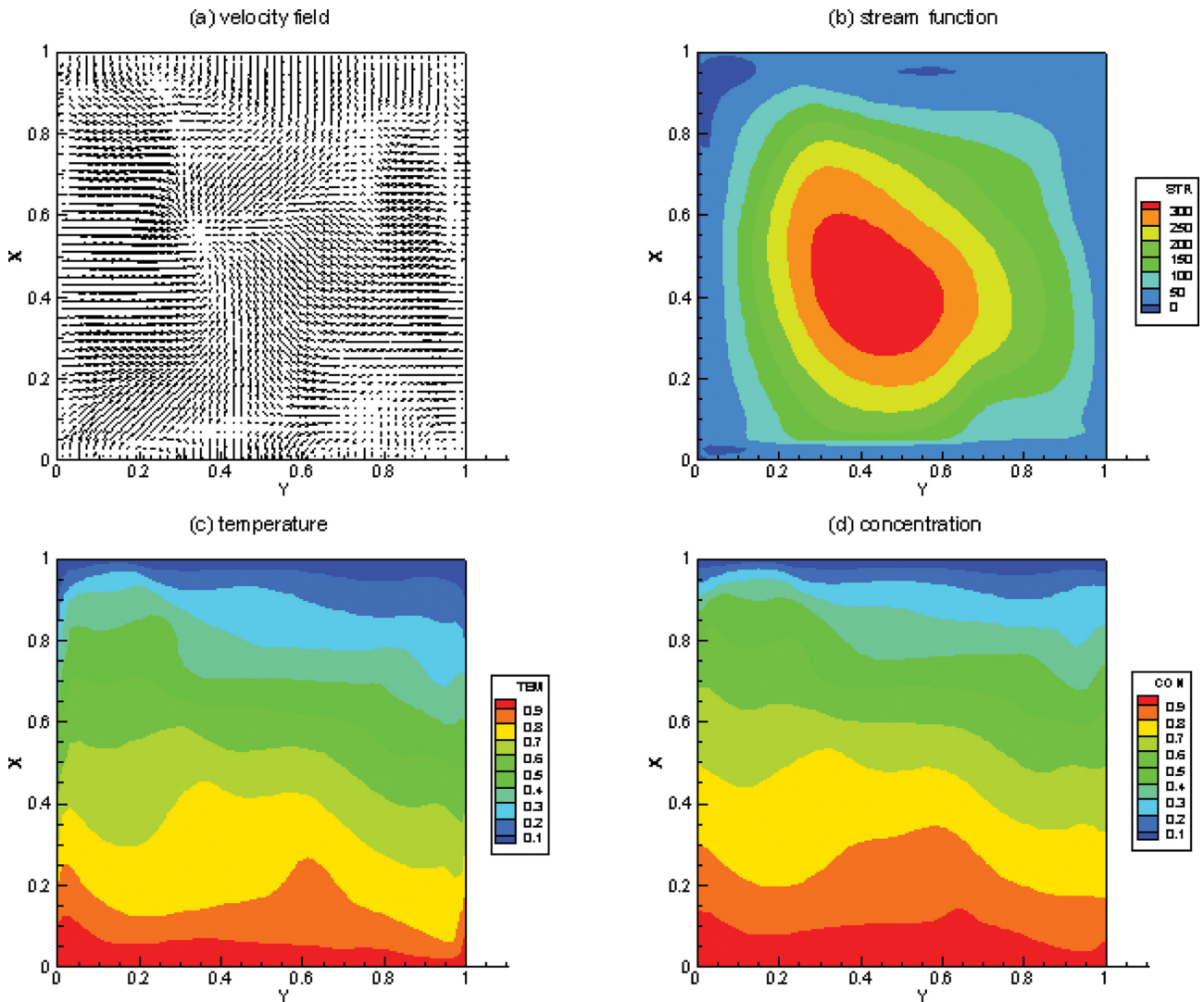


Fig. 4. Convective structures of velocity field, stream function, temperature and concentration at time (t) = 10,000 seconds. Based on aspect ratio = 1, transport length $L = 10$ cm, a linear wall temperature profile between $T_s = 623$ K and $T_c = 553$ K, thermal Rayleigh number (Ra_t) = 1.7×10^7 , solutal Rayleigh number (Ra_s) = 6.9×10^7 , Prandtl number (Pr) = 1.14, Lewis number (Le) = 0.7, Peclet number (Pe) = 1.98, concentration parameter = 1.16, partial pressure of impurity (I_2) = 100 Torr. (a) velocity field, (b) stream function ($\Delta\psi = 50$, $\psi_{\max} = 352$, $\psi_{\min} = -11.5$), (c) temperature ($\Delta T = 0.1$, $T_{\max} = 1.0$, $T_{\min} = 0$), (d) concentration ($\Delta C = 0.1$, $C_{\max} = 1.0$, $C_{\min} = 0$). A relative velocity vector with a magnitude of 1,000 has 0.8 cm. The maximum velocity vector is 7.5 cm s^{-1} .

tal Rayleigh number (Ra_s) = 6.9×10^7 , Prandtl number (Pr) = 1.14, Lewis number (Le) = 0.7, Peclet number (Pe) = 1.98, concentration parameter = 1.16, partial pressure of impurity (I_2) = 100 Torr. The four fields are given: (a) velocity field, (b) stream function ($\Delta\psi = 50$, $\psi_{\max} = 352$, $\psi_{\min} = -11.5$), (c) temperature ($\Delta T = 0.1$, $T_{\max} = 1.0$, $T_{\min} = 0$), (d) concentration ($\Delta C = 0.1$, $C_{\max} = 1.0$, $C_{\min} = 0$). A relative velocity vector with a magnitude of 1,000 has 0.8 cm, with the maximum velocity vector of 7.5 cm s^{-1} . Fig. 5 shows the convective structures of velocity field, stream function, temperature and concentration at $t = 30,000$ seconds: (a) velocity field, (b) stream function ($\Delta\psi = 50$, $\psi_{\max} = 30.6$, $\psi_{\min} = -202.89$), (c) temperature ($\Delta T = 0.1$, $T_{\max} = 1.0$,

$T_{\min} = 0$), (d) concentration ($\Delta C = 0.1$, $C_{\max} = 1.0$, $C_{\min} = 0$). A relative velocity vector with a magnitude of 1,000 has 0.16 cm, with the maximum velocity vector of 7.86 cm s^{-1} . There is found to be of little difference between both cases with respect to the magnitude of maximum velocity vector.

The other convective parameters such as $Ar = 1$, $\Delta T = 70$ K, a linear temperature profile imposed, partial pressure of impurity (I_2) = 100 Torr except both the transport length and width are 5 cm, thermal Rayleigh number and solutal Rayleigh number, are same as those in Figs. 4 and 5. The corresponding convective structures of velocity field, stream function, temperature and concentration are given in Fig. 6. The

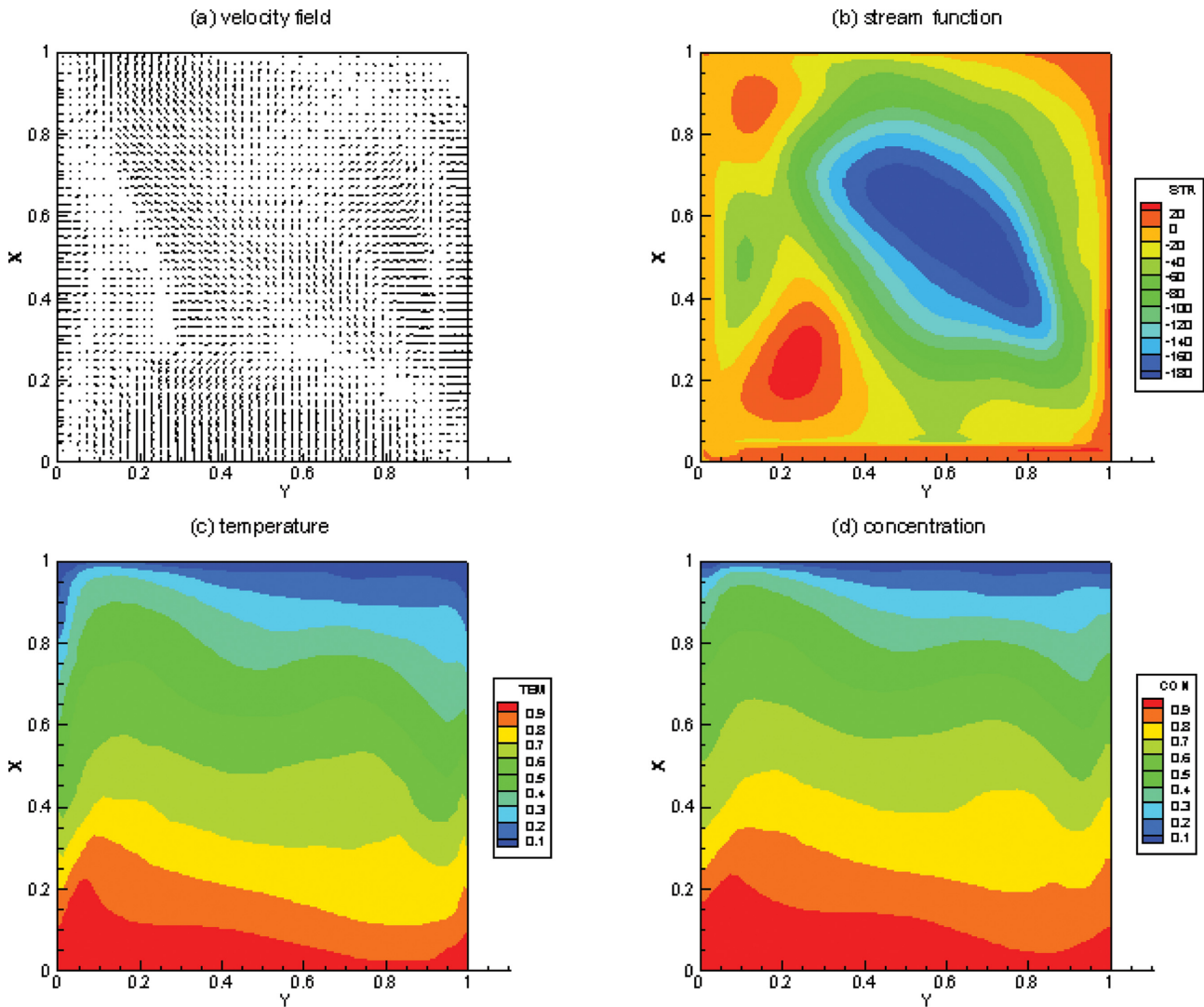


Fig. 5. Convective structures of velocity field, stream function, temperature and concentration at time (t)=30,000 seconds. (a) velocity field, (b) stream function ($\Delta\psi = 50$, $\psi_{\max} = 30.6$, $\psi_{\min} = -202.89$), (c) temperature ($\Delta T = 0.1$, $T_{\max} = 1.0$, $T_{\min} = 0$), (d) concentration ($\Delta C = 0.1$, $C_{\max} = 1.0$, $C_{\min} = 0$). A relative velocity vector with a magnitude of 1,000 has 0.16 cm. The maximum velocity vector is 7.86 cm s^{-1} .

corresponding thermal Rayleigh number $= 2.16 \times 10^6$ and solutal Rayleigh number $= 8.7 \times 10^6$ are obtained and the convergence reaches at time (t)=2,173 seconds. Fig. 6 is based on aspect ratio=1, transport length $L = 5 \text{ cm}$, a linear wall temperature profile between $T_s = 623 \text{ K}$ and $T_c = 553 \text{ K}$, thermal Rayleigh number (Ra_t) $= 2.16 \times 10^6$, solutal Rayleigh number (Ra_s) $= 8.7 \times 10^6$, Prandtl number (Pr) $= 1.14$, Lewis number (Le) $= 0.7$, Peclet number (Pe) $= 1.98$, concentration parameter $= 1.16$, partial pressure of impurity (I_2) $= 100 \text{ Torr}$. The (a) velocity field, (b) stream function ($\Delta\psi = 0$, $\psi_{\max} = 4.5$, $\psi_{\min} = -0.6$), (c) temperature ($\Delta T = 0.1$, $T_{\max} = 1.0$, $T_{\min} = 0$), (d) concentration ($\Delta C = 0.1$, $C_{\max} = 1.0$, $C_{\min} = 0$), are given. A relative velocity vector with a magnitude of 1,000 has 0.8 cm. The

maximum velocity vector is 0.14 cm s^{-1} . As shown in Fig. 6, the convective flow exhibits one-dimensional diffusional flow.

Fig. 7 shows the convective structures at $t = 5,330$ seconds, based on aspect ratio = 1 ($L = 10 \text{ cm}$), a linear wall temperature profile between $T_s = 623 \text{ K}$ and $T_c = 573 \text{ K}$ in a horizontal configuration with respect to the gravity. Fig. 7 corresponds to the cases Figs. 2 and 3. The four convective fields are given as (a) velocity field, (b) stream function ($\Delta\psi = 2$, $\psi_{\max} = 21.71$, $\psi_{\min} = 2$), (c) temperature ($\Delta T = 0.1$, $T_{\max} = 1.0$, $T_{\min} = 0$), (d) concentration ($\Delta C = 0.1$, $C_{\max} = 1.0$, $C_{\min} = 0$). A relative velocity vector with a magnitude of 100 has 1.4 cm, with the maximum velocity vector of 0.35 cm s^{-1} . In comparison with the cases of Figs. 2

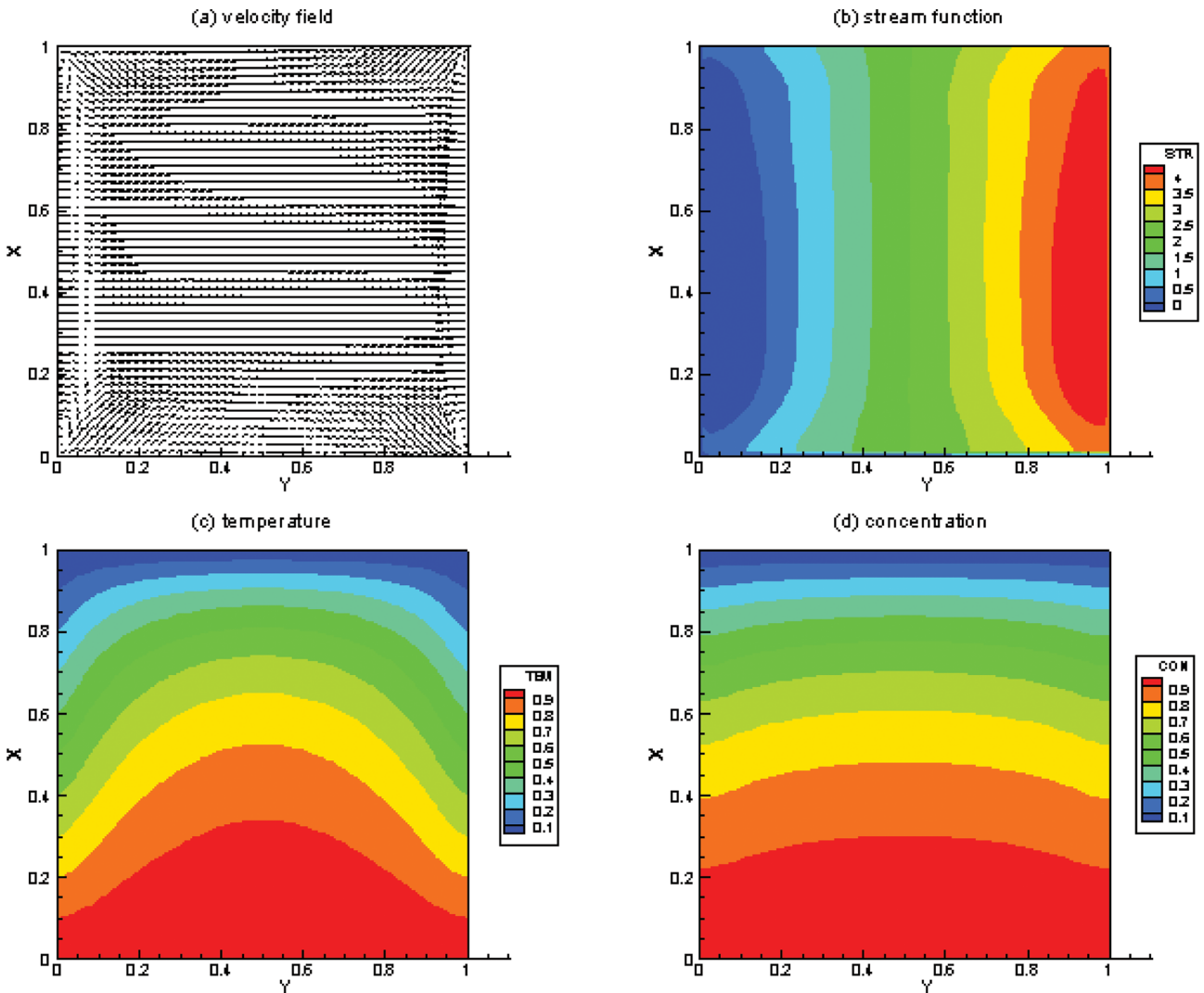


Fig. 6. Convective structures of velocity field, stream function, temperature and concentration at time $(t)=2,173$ seconds. Based on aspect ratio = 1, transport length $L=5$ cm, a linear wall temperature profile between $T_s=623$ K and $T_c=553$ K, thermal Rayleigh number $(Ra_t)=2.16 \times 10^6$, solutal Rayleigh number $(Ra_c)=8.7 \times 10^6$, Prandtl number $(Pr)=1.14$, Lewis number $(Le)=0.7$, Peclet number $(Pe)=1.98$, concentration parameter = 1.16, partial pressure of impurity $(I_2)=100$ Torr. (a) velocity field, (b) stream function ($\Delta\psi=50$, $\psi_{\max}=4.5$, $\psi_{\min}=-0.6$), (c) temperature ($\Delta T=0.1$, $T_{\max}=1.0$, $T_{\min}=0$), (d) concentration ($\Delta C=0.1$, $C_{\max}=1.0$, $C_{\min}=0$). A relative velocity vector with a magnitude of 1,000 has 0.8 cm. The maximum velocity vector is 0.14 cm s^{-1} .

and 3, the magnitude of the maximum velocity is reduced by one order of magnitude. As shown in Fig. 7(a) and (b), one main cell and one small cell occur. The four convective flow structures are asymmetrical in Fig. 7. It should be emphasized again that Fig. 7 is related to a horizontal position with respect to the gravity vector and Fig. 8 shows the schematic description of a two-dimensional PVT model for a $Hg_2Cl_2-I_2$ system.

4. Conclusions

The convective flow structures in PVT growth of

mercurous chloride crystals by the sublimation-condensation mechanism are investigated computationally. The convective flow structures are essentially time independent on the horizontal orientation of the enclosure with respect to the gravity vector, and on the other hand, time dependent on the vertical orientation of the enclosure with respect to the gravity vector. Moreover, with decreasing the thermal Rayleigh number, i.e., shortening the transport length, for the convective regime from thermal Rayleigh number of 2.16×10^6 up to 1.7×10^7 , under consideration, the convective flow has a tendency of time independent problem, and of one-dimensional diffusional flow. With time marching, the convective cells are decreased for the thermal

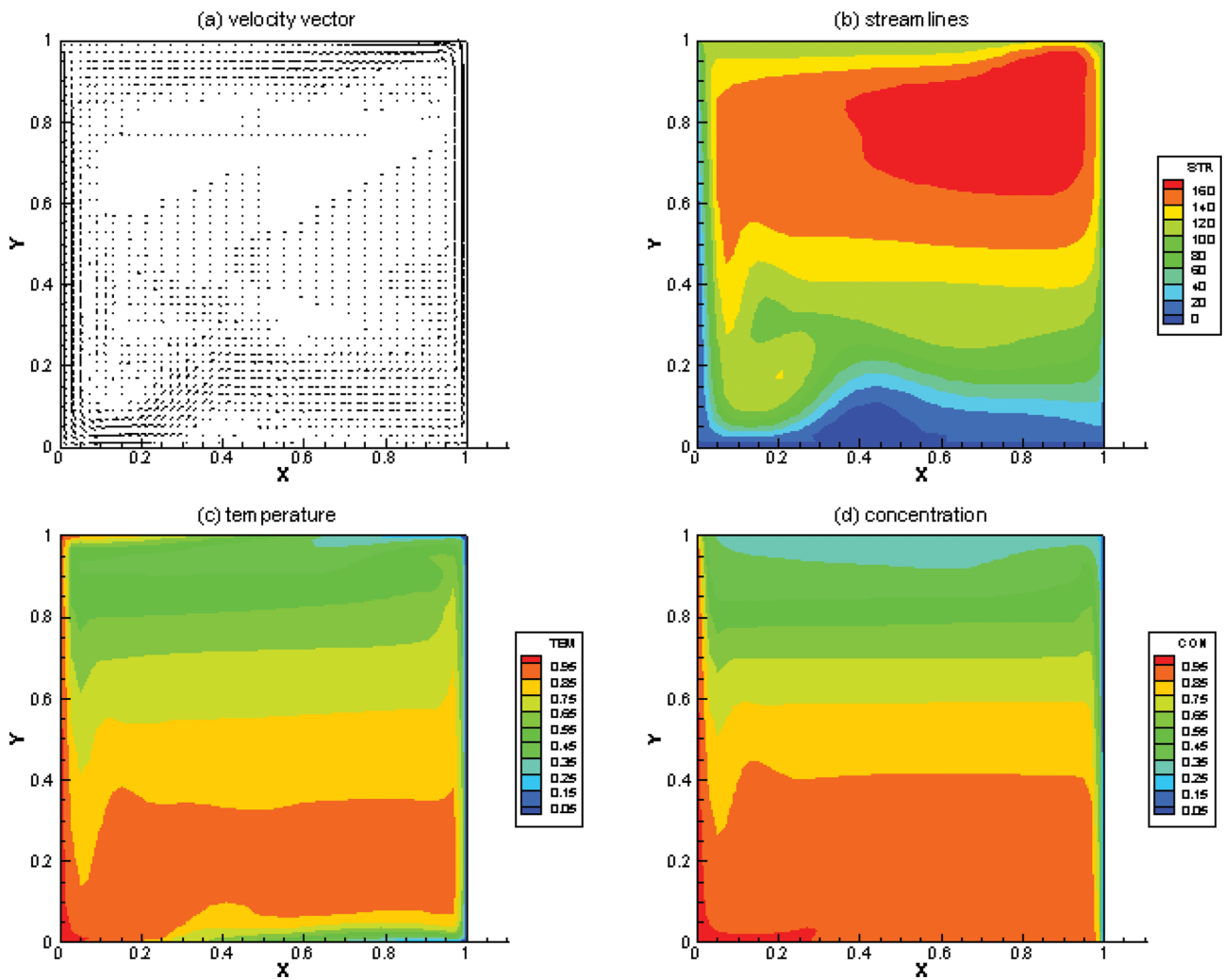


Fig. 7. Convective structures at $t=5,330$ seconds. Based on aspect ratio = 1 ($L=10$ cm), a linear wall temperature profile between $T_s=623$ K and $T_c=573$ K. (a) velocity field, (b) stream function ($\Delta\psi=2$, $\psi_{\max}=21.71$, $\psi_{\min}=2$), (c) temperature ($\Delta T=0.1$, $T_{\max}=1.0$, $T_{\min}=0$), (d) concentration ($\Delta C=0.1$, $C_{\max}=1.0$, $C_{\min}=0$). A relative velocity vector with a magnitude of 100 has 1.4 cm. The maximum velocity vector is 0.35 cm s^{-1} .

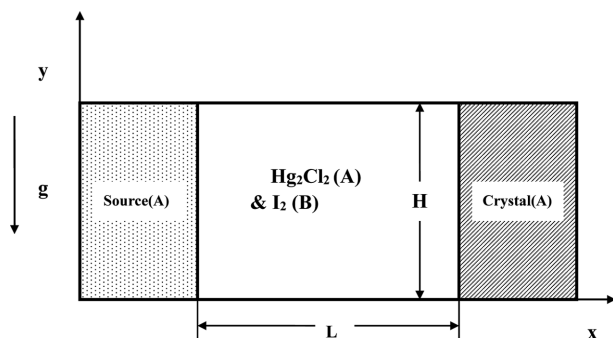


Fig. 8. Schematic description of a two-dimensional PVT model for a $\text{Hg}_2\text{Cl}_2\text{-I}_2$ system in a horizontal position with respect to the gravity vector.

Rayleigh number of 2.16×10^6 , and increased for the thermal Rayleigh number of 1.7×10^7 .

Acknowledgement

This research has been financially supported by the Hannam University through the Hannam University Kyo Bi project number 2016A037 (April 1, 2016 to March 31, 2017).

References

- [1] W.M.B. Duval, "Convective effects during the physical vapor transport process-- I: Thermal convection", J. Mater. Processing Manu. Sci. 1 (1992) 83.
- [2] W.M.B. Duval, "Convective effects during the physical vapor transport process-- II: Thermosolutal convection", J. Mater. Processing Manu. Sci. 1 (1993) 295.
- [3] W.M.B. Duval, "Transition to chaos in the physical

- vapor transport process - I, proceeding of the ASME-WAM winter Annual Meeting, Symposium in fluid mechanics phenomena in microgravity" (ASME-WAM, New Orleans, Louisiana, 1993).
- [4] W.M.B. Duval, N.B. Singh and M.E. Glicksman, "Physical vapor transport of mercurous chloride crystals: design of a microgravity experiment", *J. Cryst. Growth* 174 (1997) 120.
- [5] D.W. Greenwell, B.L. Markham and F. Rosenberger, "Numerical modeling of diffusive physical vapor transport in cylindrical Ampoules", *J. Cryst. Growth* 51 (1981) 413.
- [6] B.L. Markham, D.W. Greenwell and F. Rosenberger, "Numerical modeling of diffusive-convective physical vapor transport in cylindrical vertical ampoules", *J. Cryst. Growth* 51 (1981) 426.
- [7] A. Nadarajah, F. Rosenberger and J. Alexander, "Effects of buoyancy-driven flow and thermal boundary conditions on physical vapor transport", *J. Cryst. Growth* 118 (1992) 49.
- [8] H. Zhou, A. Zebib, S. Trivedi and W.M.B. Duval, "Physical vapor transport of zinc-telluride by dissociative sublimation", *J. Cryst. Growth* 167 (1996) 534.
- [9] F. Rosenberger, J. Ouazzani, I. Viohl and N. Buchan, "Physical vapor transport revised", *J. Cryst. Growth* 171 (1997) 270.
- [10] G.T. Kim, W.M.B. Duval, N.B. Singh and M.E. Glicksman, "Thermal convective effects on physical vapor transport growth of mercurous chloride crystals (Hg_2Cl_2) for axisymmetric 2-D cylindrical enclosure", *Modelling. Simul. Mater. Sci. Eng.* 3 (1995) 331.
- [11] G.T. Kim, W.M.B. Duval and M.E. Glicksman, "Thermal convection in physical vapour transport of mercurous chloride (Hg_2Cl_2) for rectangular enclosures", *Modelling. Simul. Mater. Sci. Eng.* 5 (1997) 289.
- [12] P.A. Tebbe, S.K. Loyalka and W.M.B. Duval, "Finite element modeling of asymmetric and transient flow fields during physical vapor transport", *Finite Elem. Anal. Des.* 40 (2004) 1499.
- [13] G.T. Kim and M.H. Kwon, "Numerical analysis of the influences of impurity on diffusive-convection flow fields by physical vapor transport under terrestrial and microgravity conditions: with application to mercurous chloride", *App. Chem. Eng.* 27 (2016) 335.
- [14] S.V. Patankar, "Numerical heat transfer and fluid flow" (Hemisphere Publishing Corp., Washington D.C., 1980).
- [15] A. Nakayama, "PC-aided numerical heat transfer and convective flow" (CRC press., Tokyo, 1995).